

# LIME-LLM: Probing Models with Fluent Counterfactuals, Not Broken Text

**George Mihaila**  
 University of North Texas  
 georgemihaila@my.unt.edu

**Himanshu Sharma**  
 University of North Texas  
 himanshusharma@my.unt.edu

**Suleyman Olcay Polat**  
 University of North Texas  
 suleymanolcaypolat@my.unt.edu

**Namratha V. Urs**  
 University of North Texas  
 namrathaurs@my.unt.edu

**Poli Nemkova**  
 University of North Texas  
 poli.nemkova@unt.edu

**Mark V. Albert**  
 University of North Texas  
 mark.albert@unt.edu

## Abstract

Local explanation methods such as LIME (Ribeiro et al., 2016) remain fundamental to trustworthy AI, yet their application to NLP is limited by a reliance on random token masking. These heuristic perturbations frequently generate semantically invalid, out-of-distribution inputs that weaken the fidelity of local surrogate models. While recent generative approaches such as LLiMe (Angiulli et al., 2025b) attempt to mitigate this by employing Large Language Models for neighborhood generation, they rely on unconstrained paraphrasing that introduces confounding variables, making it difficult to isolate specific feature contributions. We introduce LIME-LLM, a framework that replaces random noise with hypothesis-driven, controlled perturbations. By enforcing a strict "Single Mask–Single Sample" protocol and employing distinct neutral infill and boundary infill strategies, LIME-LLM constructs fluent, on-manifold neighborhoods that rigorously isolate feature effects. We evaluate our method against established baselines (LIME, SHAP, Integrated Gradients) and the generative LLiMe baseline across three diverse benchmarks: CoLA, SST-2, and HateXplain using human-annotated rationales as ground truth. Empirical results demonstrate that LIME-LLM establishes a new benchmark for black-box NLP explainability, achieving significant improvements in local explanation fidelity compared to both traditional perturbation-based methods and recent generative alternatives.

## 1 Introduction

*"The problem is not that machines think like humans, but that humans think machines think like humans."*

— Herbert A. Simon

As large language models (LLMs) and transformer-based classifiers have become central to NLP, the need for transparent and trustworthy explanations has grown accordingly (Doshi-Velez

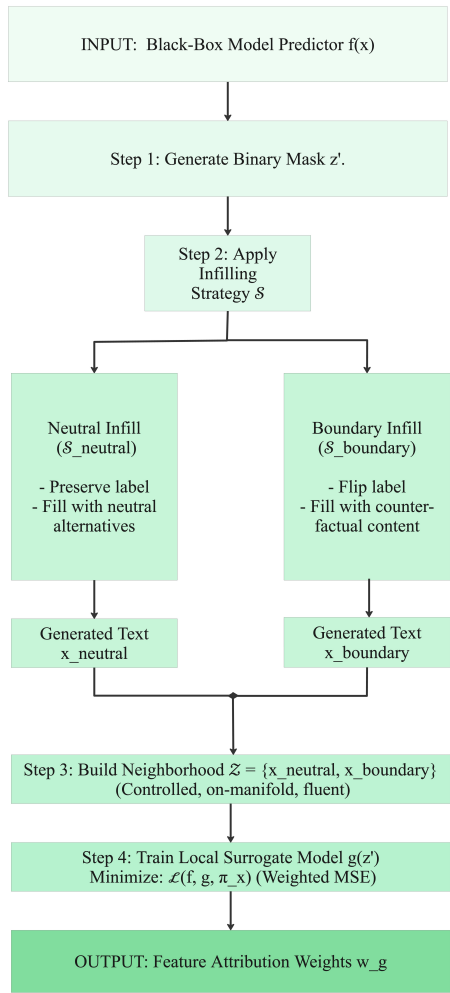


Figure 1: Overview of the proposed LIME-LLM framework. LIME-LLM constructs local neighborhoods using hypothesis-driven, on-manifold LLM infilling, generating one fluent sample per binary mask via label-preserving neutral or counterfactual boundary strategies. The resulting semantic neighborhood enables faithful local surrogate explanations.

and Kim, 2017; Narayanan et al., 2018). Among model-agnostic methods, LIME (Ribeiro et al., 2016) remains widely used due to its simplicity and generality. However, in textual settings, LIME

constructs local neighborhoods via random token masking, often producing ungrammatical and semantically implausible perturbations that lie far from the data manifold, a limitation repeatedly documented in diagnostic studies (Atanasova et al., 2020; Jacovi and Goldberg, 2020).

Such “broken” inputs lead to unstable explanations and misleading feature attributions (Yeh et al., 2019; Slack et al., 2020). The issue is particularly acute for tasks where meaning depends on multi-token interactions, including toxicity detection (Mathew et al., 2021), socially nuanced language (Nemkova et al., 2023), and linguistic acceptability, where masking individual tokens often destroys the semantic structure required for reliable local surrogate modeling.

Prior work has sought to improve perturbation-based explanations through phrase-level masking (Zhou et al., 2025a) and syntactic constraints (Amara et al., 2024). While these approaches improve robustness in specific settings, they typically require additional linguistic resources and remain confined to token-deletion-based perturbation spaces. In parallel, recent work has begun incorporating LLMs into local surrogate frameworks to generate fluent, on-manifold neighborhoods. Notably, LLiMe (Angiulli et al., 2025a) employs LLM-based paraphrasing to construct perturbations. However, unconstrained paraphrasing often alters multiple linguistic factors - syntax, lexical choice, and tone - simultaneously, introducing confounding variables that hinder precise feature attribution.

Other directions include game-theoretic attribution (Lundberg and Lee, 2017a), rule-based anchoring (Ribeiro et al., 2018a), and latent-space generation (Lampridis et al., 2022b), each with distinct tradeoffs between fidelity, coherence, and computational cost.

In this work, we introduce LIME-LLM, a framework that addresses the tension between semantic validity and feature isolation (Figure 1). LIME-LLM enforces a strict Single Mask–Single Sample protocol, decoupling hypothesis specification from text generation. For each fixed binary feature mask, the LLM is used strictly as a semantic infiller, generating exactly one controlled perturbation per hypothesis.

We evaluate LIME-LLM against standard model-agnostic baselines, including LIME (Ribeiro et al., 2016) and SHAP, as well as the recent generative baseline LLiMe (Angiulli et al., 2025a). Across

global and local evaluation criteria, we show that controlled, hypothesis-driven infilling yields more stable and plausible explanations than either random perturbation or unconstrained generation.

Our results demonstrate that semantic neighborhood construction is a central bottleneck in perturbation-based NLP explainability and that LLM-guided perturbations offer a practical, model-agnostic solution. Empirically, LIME-LLM outperforms standard LIME by 34–135% in ROC-AUC across tasks and frequently exceeds even white-box Integrated Gradients, despite requiring no access to model internals. By improving explanation faithfulness and stability without sacrificing deployment flexibility, LIME-LLM advances the reliability of local explanations for modern NLP models.

To facilitate reproducibility and community adoption, we release our implementation as an open-source Python package.<sup>1</sup>

## 2 Related Work

Our work builds on extensive research in post-hoc explainability for NLP, broadly categorized into gradient-based, perturbation-based, and generative model-based methods, which differ in model access assumptions, explanation fidelity, and robustness.

Gradient-based approaches assign token-level importance via model gradients. Methods such as SignedGI (Du and Xu, 2021) and Integrated Gradients (Sundararajan et al., 2017) provide high-fidelity explanations for Transformer classifiers (Zheng and Pamuksuz, 2024) when model internals are accessible, but are inapplicable in black-box or proprietary settings (Jacovi and Goldberg, 2020).

Perturbation-based methods infer importance by modifying inputs and observing prediction changes. LIME (Ribeiro et al., 2016) remains the canonical example, with extensions such as PR-LIME (Zhou et al., 2025b), XPROB (Cai et al., 2024), and MExGen (Paes et al., 2024) improving phrase coherence, stability, or applicability to generative models. Nonetheless, many still generate semantically implausible neighborhoods, especially for longer or compositional texts.

A parallel line of work addresses the instability of LIME-style explanations, which are sensitive to sampling, kernel width, and surrogate fitting (Yeh et al., 2019; Slack et al., 2020). Proposed stabilizations include deterministic or clustered neighborhoods DLIME (Zafar and Khan, 2019),

---

<sup>1</sup>The repository URL will be provided upon acceptance.

hypothesis-testing-based methods S-LIME (Zhou et al., 2021), Bayesian surrogates BayLIME (Zhao et al., 2021), and revised sampling or weighting schemes GLIME (Tan et al., 2023), OptiLIME (Visani et al., 2020)), all aiming to reduce variance (Angiulli et al., 2025a). However, these methods typically retain token-masking perturbations and thus inherit LIME’s semantic limitations.

Syntax-aware methods explicitly incorporate linguistic structure. SyntaxShap (Amara et al., 2024) constrains Shapley coalitions using dependency parses, yielding more coherent explanations for autoregressive models such as GPT-2 and Mistral-7B, but typically relies on external parsers and structured representations. Related work also includes SIDU-TXT (Jahromi et al., 2024), which adapts visual explanation techniques to text, and rule-based grouping approaches such as Anchors (Ribeiro et al., 2018b).

Generative model-based approaches aim to produce more realistic neighborhoods by sampling from learned latent spaces. Examples include *xspells* (Lampridis et al., 2022a), which uses variational autoencoders to generate exemplars and counter-exemplars, and XPROA (Cai et al., 2023), which applies generative interpolation to approximate local decision boundaries. These methods improve coherence but often require additional training or architectural assumptions.

Most recently, LLM-generated neighborhoods have emerged as a promising alternative. LLiMe (Angiulli et al., 2025a) replaces token masking with classifier-driven LLM generation to produce semantically coherent perturbations. While LLiMe mitigates the out-of-distribution problem, it relies on unconstrained paraphrasing that alters multiple linguistic factors simultaneously, introducing confounding variables. We include LLiMe as a generative baseline to demonstrate the advantages of our controlled Single Mask–Single Sample protocol.

### 3 Methodology

We propose LIME-LLM, a model-agnostic explanation framework that addresses the semantic limitations of standard perturbation-based methods. Unlike LIME, which generates local neighborhoods via token deletion, LIME-LLM employs a controlled, hypothesis-driven generation process using LLMs. This approach ensures that all neighborhood samples remain on the data manifold while maintaining the feature isolation necessary

for faithful linear approximation.

#### 3.1 Preliminaries and Problem Formulation

Let  $f : \mathcal{X} \rightarrow [0, 1]^C$  be a black-box text classifier that maps an input sequence  $x = \{w_1, \dots, w_d\}$  to a probability distribution over  $C$  classes. Given a specific instance  $x$ , LIME seeks to approximate  $f$  locally using an interpretable linear model  $g(z') = w_g \cdot z'$ , where  $z' \in \{0, 1\}^d$  is a binary vector representing the presence or absence of tokens.

In LIME, a neighborhood  $\mathcal{Z}$  is constructed by randomly sampling  $N$  binary masks  $z'_i$ . The corresponding textual representation  $z_i$  is created by deleting tokens where  $z'_{i,j} = 0$ . We denote this mapping as  $h_{del}(x, z')$ . The surrogate  $g$  is then trained to minimize the weighted squared loss:

$$\mathcal{L}(f, g, \pi_x) = \sum_{z'_i \in \mathcal{Z}} \pi_x(z_i) (f(z_i) - g(z'_i))^2 \quad (1)$$

where  $\pi_x(z_i)$  is a proximity kernel (typically exponential cosine distance).

**The Manifold Problem:** A critical failure mode in NLP is that  $h_{del}(x, z')$  frequently yields out-of-distribution (OOD) text (e.g., “The movie was bad” to “movie bad”). Since  $f$  was trained on natural text, its predictions on OOD inputs such as  $f(z_i)$  are unreliable, introducing noise into Eq. 1 and degrading the fidelity of  $g$ .

#### 3.2 The LIME-LLM Framework

LIME-LLM replaces the deletion operator  $h_{del}$  with a generative operator  $G_{LLM}(x, z', \mathcal{S})$ , where  $\mathcal{S}$  denotes a specific infilling strategy. Our goal is to generate a neighborhood where every sample  $x_{new}$  is fluent and on-manifold ( $x_{new} \in \mathcal{M}$ ), yet strictly corresponds to the binary hypothesis  $z'$ .

**The Single Mask - Single Sample Protocol:** Recent generative approaches like LLiMe (Angiulli et al., 2025a) rely on unconstrained paraphrasing to generate neighborhoods. This introduces feature collinearity: if a paraphrase alters syntax, tone, and vocabulary simultaneously, the linear model cannot isolate the marginal contribution of any single feature. To resolve this, we enforce a one-to-one correspondence between the hypothesis space and the text space. For every generated sample  $i$ :

1. We sample a unique binary mask  $z'_i$ .
2. We generate exactly one text sample  $x_i = G_{LLM}(x, z'_i, \mathcal{S})$ .

3. We enforce that tokens corresponding to  $z'_{i,j} = 1$  (anchors) are preserved verbatim, while  $z'_{i,j} = 0$  (masked slots) are infilled.

### 3.3 Hypothesis-Driven Infilling Strategies

To robustly map the decision boundary, we employ two distinct strategies  $\mathcal{S}$  that guide the LLM’s generation process:

1. Neutral Infill ( $\mathcal{S}_{neutral}$ ): This strategy probes the robustness of the anchor features. The LLM is instructed to infill masked slots ( $z' = 0$ ) with contextually appropriate alternatives that *preserve* the original predicted label  $y_{pred} = \text{argmax } f(x)$ .

$$x_{neutral} \sim P_{LLM}(\cdot | x_{masked}, \text{label} = y_{pred}) \quad (2)$$

This strategy populates the interior of the local decision cluster, stabilizing the intercept of the surrogate model.

2. Boundary Infill ( $\mathcal{S}_{boundary}$ ): This strategy acts as a decision boundary probe. The LLM is instructed to infill masked slots with alternatives that push the prediction toward a counterfactual label  $y_{target} \neq y_{pred}$ .

$$x_{boundary} \sim P_{LLM}(\cdot | x_{masked}, \text{label} = y_{target}) \quad (3)$$

Significantly, our strategy leverages intelligent masking, which prioritizes the masking of tokens with high prior attribution, such as strong sentiment words, to enable the LLM to effectively reassign labels by providing ample semantic flexibility.

**Avoiding the Infilling Trap:** A common failure mode in generative XAI is the tendency of LLMs to prioritize fluency over valid label flips (e.g., replacing “terrible” with “poor” instead of “great”). We mitigate this via negative constraints in the prompt, explicitly forbidding synonyms for masked high-importance tokens when  $\mathcal{S}_{boundary}$  is active.

### 3.4 Local Surrogate Optimization

Once the neighborhood  $\mathcal{N} = \{(z'_i, x_i)\}_{i=1}^N$  is generated, we obtain predictions  $f(x_i)$  from the black-box classifier. The linear surrogate  $g$  is trained by solving:

$$\hat{w}_g = \underset{w}{\text{argmin}} \sum_{i=1}^N \pi_x(x_i) (f(x_i) - w \cdot z'_i)^2 + \Omega(w) \quad (4)$$

### 3.5 Hybrid Proximity Kernel

LIME weights samples using cosine distance on sparse Bag-of-Words (BoW) vectors, which captures lexical overlap but misses semantic proximity. To better capture the decision boundaries of transformer-based models, LIME-LLM employs a hybrid proximity kernel that combines lexical and semantic signals:

$$\pi_x(x_i) = \frac{1}{2} (\text{CosSim}_{bow}(x, x_i) + \text{CosSim}_{emb}(x, x_i)) \quad (5)$$

where  $\text{CosSim}_{bow}$  measures surface-level token overlap and  $\text{CosSim}_{emb}$  measures dense semantic similarity using sentence embeddings. This hybrid weighting ensures that perturbations are penalized not just for changing words, but for drifting from the original semantic meaning. The specific embedding model is detailed in Section 4.4.

## 4 Experiments

To systematically evaluate LIME-LLM, we performed experiments on three diverse text classification benchmarks using BERT-base classifiers (Devlin et al., 2019). We compare our approach against perturbation-based, gradient-based, and generative explanation methods.

### 4.1 Datasets and Sampling Protocol

We utilized the following datasets representing three distinct linguistic challenges: sentiment analysis, toxicity detection, and linguistic acceptability.

1. **CoLA** (Warstadt et al., 2019): A binary acceptability task, with a focus on *Unacceptable* sentences to test the method’s ability to pinpoint subtle syntactic violations (e.g., subject-verb disagreement).
2. **SST-2** (Socher et al., 2013): Binary sentiment classification. Tests the attribution of sentiment-bearing adjectives and modifiers.
3. **HateXplain** (Mathew et al., 2021): A 3-class toxic language task, with a focus on the *Hate* and *Offensive* classes to test sensitivity to context and slurs.

For our final evaluation, we constructed a stratified test set of 150 instances, consisting of 50 samples from each dataset. We prioritize annotation quality over scale, following established practice in

human-centered XAI evaluation (DeYoung et al., 2019). To ensure that our explanations address the most critical use cases for interpretability, we applied strict filtering criteria during sample selection:

- **Correctness Constraint:** We selected only instances that were correctly predicted by the black-box classifier. This ensures that our evaluation measures the method’s ability to explain the model’s valid decision logic rather than its error modes.
- **Utility Constraint (Class Filtering):** We restricted evaluation to classes where the need for explanation is highest. For CoLA, we selected only Unacceptable examples. In detailed linguistic analysis, it is more valuable to explain why a sentence is broken (locating the error) than to explain why a sentence is correct. For SST-2, we utilized balanced Positive/Negative samples. For HateXplain, we excluded the Normal class, focusing exclusively on Hate and Offensive speech. The primary utility of explainable AI in moderation systems is to justify flags for toxicity, not to explain benign content.

All test instances are evaluated against human-annotated token-level rationales. For HateXplain, we use the provided ground truth; for SST-2 and CoLA, which lack native token-level labels, we collected human annotations for the test samples (details in Appendix B)<sup>2</sup>.

**Prompt Tuning & Development Protocol:** To ensure generalizability, we employed a unified prompt template<sup>3</sup> across all tasks, adapting to specific domains solely through a modular {dataset\\_description} field. We maintained strict train-test separation by optimizing these descriptions on a development set drawn exclusively from the training splits. Since SST-2 and CoLA lack token-level rationales in their training data, we generated synthetic rationales using Claude Sonnet 4.5 (Anthropic, 2025). This generation pipeline was systematically calibrated on HateXplain and refined using a 30-example seed set. We leveraged these development samples to iteratively fine-tune the {dataset\_description} instructions -

<sup>2</sup>Annotation guidelines provided in the repository, URL will be provided upon acceptance.

<sup>3</sup>Full prompt can be found in the repository, URL will be provided upon acceptance.

Dataset	Train	Test	Annotation
CoLA	50	50	Human (2, $\alpha=0.64$ )
SST-2	50	50	Human (2, $\alpha=0.84$ )
HateXplain	50	50	Human (3, $\alpha=0.46$ )

Table 1: Dataset splits for development and evaluation.

verifying that the LLM correctly distinguished between neutral\_infill (label-preserving) and boundary\_infill (counterfactual) logic, before freezing the prompts for the final evaluation on the human-annotated test set. For the final assessment, the test sets were independently labeled by two human annotators, achieving substantial inter-annotator agreement (Table 1); complete annotation methodology and reliability analyses are detailed in Appendix B.

## 4.2 Baseline Methods

We compare LIME-LLM against four representative baselines:

1. LIME (Ribeiro et al., 2016): The standard model-agnostic baseline using random token deletion. We use the official implementation with default parameters (kernel width  $\sigma = 0.75$ ).
2. SHAP (Lundberg and Lee, 2017b): A game-theoretic approach that estimates Shapley values via subset sampling (token deletion).
3. Integrated Gradients (IG) (Sundararajan et al., 2017): A white-box gradient attribution method. We include IG as an upper-bound reference for fidelity, assuming access to model internals.
4. LLiMe (Angiulli et al., 2025a): The primary generative baseline. LLiMe utilizes an LLM to generate neighborhood samples via unconstrained paraphrasing. This comparison highlights the impact of our “Single Mask - Single Sample” protocol versus free-form generation.

## 4.3 Evaluation Metrics

We assess explanation quality by measuring how well the derived feature attributions align with human ground-truth rationales.

### Decision Boundary Mapping (ROC-AUC):

This is our primary metric for global alignment. We treat feature attribution as a ranking problem,

computing the Area Under the Receiver Operating Characteristic Curve (ROC-AUC) by comparing the attribution scores against binary human rationales. A higher ROC-AUC indicates that the method correctly assigns higher importance to tokens that humans deem critical to the label. This metric is robust to the scale of the weights and focuses on relative ordering.

**Precision-Recall (PR-AUC):** We also report the Area Under the Precision-Recall Curve (PR-AUC). Unlike ROC-AUC, PR-AUC is highly sensitive to the sparsity of the explanation. This metric allows us to analyze the “*Manifold Trade-off*” (Feng et al., 2018): while deletion-based methods, such as LIME, often isolate single words (high precision, low recall), on-manifold methods, like LIME-LLM, tend to attribute importance to broader semantic units or phrases (lower precision against sparse human masks, but often higher semantic validity).

#### 4.4 Implementation Details

For LIME-LLM, we utilize Claude Sonnet 4.5 as the backbone for the sample generation. We generate  $N = 20$  samples per instance, split evenly between  $\mathcal{S}_{neutral}$  and  $\mathcal{S}_{boundary}$ . While (Angiulli et al., 2025a) suggest a “sweet spot” of approximately 30 samples for generative samples, we found that our controlled, hypothesis-driven protocol converges more rapidly than free-form paraphrasing. We achieve high performance with just 20 samples, significantly lowering LLM inference costs and latency while minimizing the risk of prompt drift often observed in larger generation batches. For the semantic component of the proximity kernel, we utilize all-mpnet-base-v2 (Reimers and Gurevych, 2019), selected for its strong performance on semantic similarity benchmarks. For the LLM ablation study, we additionally evaluate performance using GPT-4.1 (Achiam et al., 2023) and Gemini 3 Flash (DeepMind, 2024) to determine if the method’s effectiveness is contingent on a specific model architecture discussed in (Additional details in Appendix A).

### 5 Results and Discussion

We evaluate the performance of LIME-LLM against LIME, Partition SHAP, Integrated Gradients (IG), and LLM. Figure 2 and Table 2 summarize the Area Under the Curve (AUC) for both ROC and Precision-Recall (PR) metrics across all three datasets.

#### 5.1 Alignment with Human Rationales (ROC-AUC)

LIME-LLM consistently achieves the highest ROC-AUC scores across all three benchmarks, outperforming LIME by substantial margins (+34% on SST-2, +87% on HateXplain, +135% on CoLA).

**Comparison with White-Box Methods.** Notably, LIME-LLM outperforms Integrated Gradients (IG), a method with access to model internals. On SST-2, LIME-LLM achieves an ROC-AUC of **0.681** compared to IG’s 0.665. Similarly, on CoLA, it achieves **0.598** versus IG’s 0.540. This suggests that probing transformer-based classifiers with linguistically valid counterfactuals can provide a better map of the decision boundary than tracing gradients.

**Controlled vs. Unconstrained Generation:** The comparison with LLM highlights the importance of our “Single Mask - Single Sample” protocol. While LLM improves over LIME on syntax tasks (CoLA ROC 0.391), it lags significantly behind LIME-LLM on semantic tasks (SST-2 ROC 0.439 vs 0.681). This confirms that unconstrained paraphrasing (LLM) introduces confounding variables that obscure the decision boundary, whereas LIME-LLM’s controlled infilling strictly isolates feature contributions.

**The Manifold Trade-off (Precision vs. Ranking):** While LIME-LLM dominates in ranking metrics (ROC-AUC), Precision-Recall (PR-AUC) scores reveal an intrinsic trade-off between semantic validity and sparsity.

As observed in Table 2, white-box methods like IG typically achieve higher PR-AUC (0.483 on SST-2 and 0.491 on HateXplain) than generative methods. This discrepancy arises from the explanation style:

- Gradient methods are pinpoint-sparse: They attribute importance to single tokens (e.g., “bad”), overlapping perfectly with sparse human masks.
- Generative methods are semantically diffuse: To maintain fluency, methods like LIME-LLM and LLM perturb entire phrases. Consequently, importance is distributed across the phrase, lowering token-level precision.

This effect is most severe for LLM (PR 0.261 on CoLA), where unconstrained paraphrasing drifts far from the original lexical structure. LIME-LLM

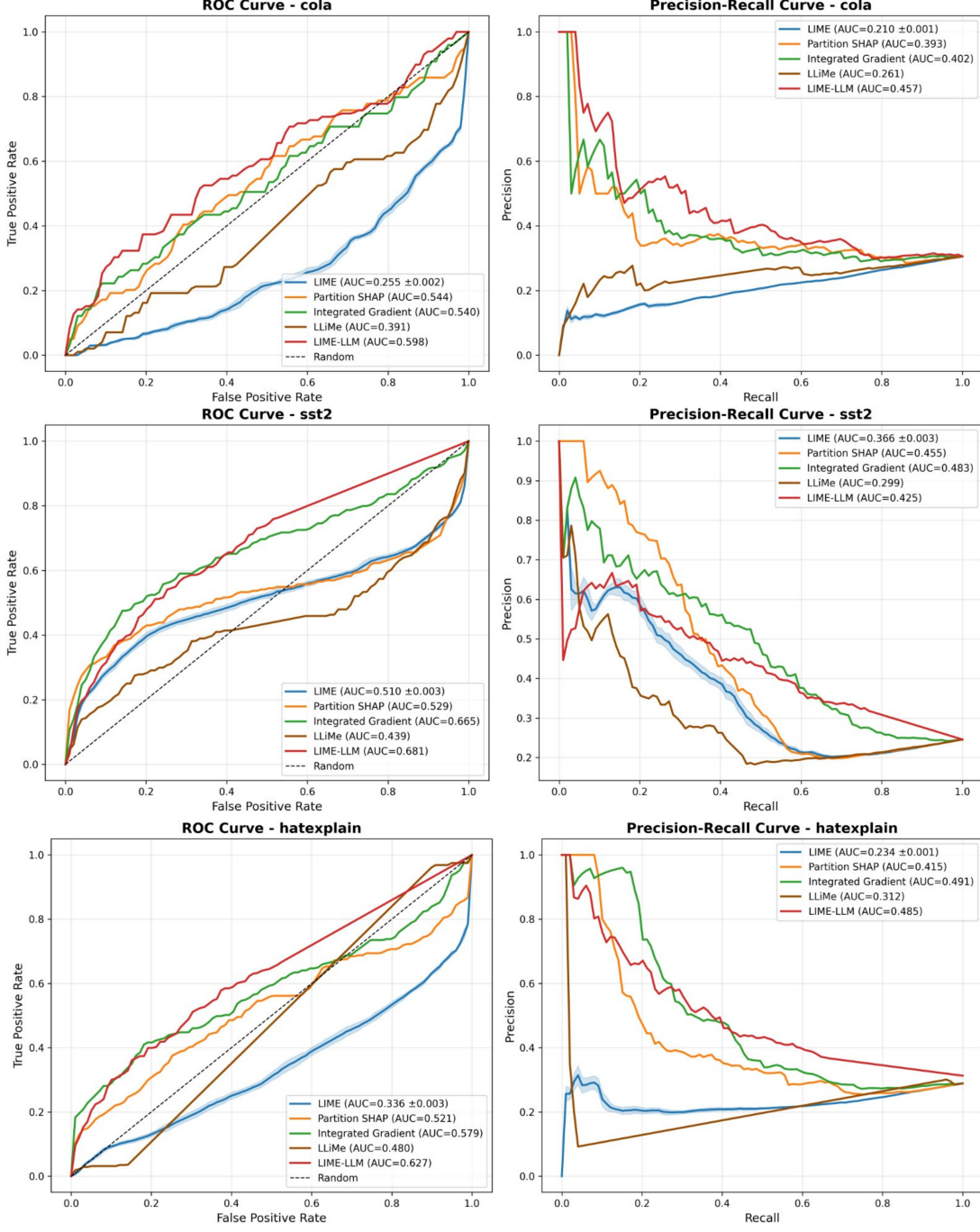


Figure 2: Comparison of ROC and Precision-Recall (PR) curves across three evaluation datasets: CoLA (top), SST-2 (middle), and HateXplain (bottom). Shaded regions indicate 95% confidence intervals over 30 random seeds for stochastic methods. LIME-LLM consistently outperforms LIME and Partition SHAP, and achieves faithfulness comparable to Integrated Gradients while remaining fully model-agnostic.

(PR 0.457 on CoLA) mitigates this by anchoring the generation, striking a better balance between manifold validity and feature localization.

## 5.2 Task-Specific Analysis

**SST-2 (Semantics):** LIME-LLM achieves its strongest gains here (ROC 0.681). The gap between

LIME-LLM and LLiMe (ROC 0.439) is widest on this task, indicating that sentiment analysis requires precise, localized counterfactuals (e.g., flipping adjectives) rather than whole-sentence paraphrases.

**HateXplain (Context):** Toxicity detection often depends on specific trigger words. While LIME (ROC 0.336) fails because deleting a slur renders

Method	SST-2 (Sentiment)		HateXplain (Toxicity)		CoLA (Syntax)	
	ROC $\uparrow$	PR $\uparrow$	ROC $\uparrow$	PR $\uparrow$	ROC $\uparrow$	PR $\uparrow$
LIME (Standard)	$0.510 \pm 0.003$	$0.366 \pm 0.003$	$0.336 \pm 0.003$	$0.234 \pm 0.001$	$0.255 \pm 0.002$	$0.210 \pm 0.001$
Partition SHAP	<b>0.529</b>	0.455	0.521	0.415	0.544	0.393
Integrated Gradients	0.665	<b>0.483</b>	0.579	<b>0.491</b>	0.540	0.402
LLiMe (Generative)	0.439	0.299	0.480	0.312	0.391	0.261
<b>LIME-LLM (Ours)</b>	<b>0.681</b>	0.425	<b>0.627</b>	0.485	<b>0.598</b>	<b>0.457</b>

Table 2: Comparison of explanation fidelity across datasets. ROC-AUC measures ranking alignment with human rationales; PR-AUC measures sparsity-adjusted precision. Best black-box results in bold. Mean  $\pm$  95% confidence intervals reported for LIME over 30 random seeds to account for its stochastic nature.

text nonsensical, LIME-LLM (ROC 0.627) successfully replaces slurs with neutral concepts. LLiMe (ROC 0.480) shows improvement over LIME but lags behind LIME-LLM, possibly because unconstrained paraphrasing of toxic content may trigger LLM safety filters or alter contextual cues beyond the intended label manipulation. LLiMe failed to produce valid explanations for 86% of HateXplain instances (vs. 0% on SST-2, 4% on CoLA), likely due to safety filters blocking toxic paraphrases.

**CoLA (Syntax):** This task validates the "on-manifold" hypothesis. Both generative methods - LIME-LLM (ROC 0.598, PR 0.457) and LLiMe (ROC 0.391, PR 0.261) - drastically outperform Standard LIME (ROC 0.255, PR 0.210). Since CoLA measures linguistic acceptability, "broken" deletion-based samples provide no signal. The success of LLiMe here suggests that for syntax, any fluent perturbation is better than noise, though LIME-LLM's controlled infilling still yields the best fidelity.

## 6 Ablation Study

To assess the robustness of LIME-LLM, we perform controlled ablations on two key components: the generative backbone and the locality weighting function. Table 3 summarizes the results across all datasets.

### 6.1 Backbone Model Sensitivity

Replacing Claude Sonnet 4.5 with GPT-4.1 (OpenAI, 2024) and Gemini 3 Flash (DeepMind, 2024) confirms that our gains are not model-specific. While absolute scores vary, relative improvements remain robust: even when using lower-performing backbones (e.g., GPT-4.1 on semantic tasks), LIME-LLM significantly outperforms Standard LIME on SST-2, while Gemini 3 Flash surpasses the white-box Integrated Gradients baseline on HateXplain (ROC 0.659). This demonstrates that

LIME-LLM's efficacy stems from the hypothesis-driven protocol rather than the idiosyncrasies of a single LLM.

## 6.2 Distance Metric Sensitivity

We evaluate three neighborhood weighting kernels: (1) BoW (sparse lexical cosine), (2) Embedding (dense semantic cosine), and (3) Hybrid (arithmetic mean). The Hybrid weighting consistently improves fidelity, confirming that the surrogate must penalize both lexical deviation (BoW) and semantic drift (Embedding) to accurately map the transformer's decision boundary. Full tabulation of results for both ablation studies can be found in Appendix A.

## 7 Conclusion

Standard perturbation-based explainers suffer from a fundamental validity problem: probing models with broken, OOD text. We presented LIME-LLM, a framework that addresses this by replacing random deletion with hypothesis-driven semantic infilling. Our key insight is the "Single Mask–Single Sample" protocol, which decouples hypothesis specification from text generation, enabling controlled perturbations that remain fluent while strictly isolating feature contributions. Through complementary neutral and boundary infill strategies, LIME-LLM constructs on-manifold neighborhoods that probe both the interior and boundaries of local decision regions. Empirically, LIME-LLM outperforms standard LIME by 34–135% in ROC-AUC across sentiment, toxicity, and syntax tasks, and frequently exceeds white-box Integrated Gradients despite requiring no model internals. Our results suggest that semantic neighborhood construction, not surrogate model complexity, is the central bottleneck in perturbation-based NLP explainability.

## Limitations

While LIME-LLM substantially improves the semantic validity and stability of local explanations for text, several limitations remain:

1. **Computational Cost.** LLM-guided neighborhood construction incurs higher computational overhead than token-deletion-based methods, which may limit scalability in large-scale or latency-sensitive settings. To mitigate this, LIME-LLM employs a batched prompting strategy in which multiple perturbations are generated within a single LLM invocation. In our experiments, each explanation uses one structured prompt to produce 20 hypothesis-driven perturbations, resulting in 150 total LLM calls for 150 explained instances. While this design substantially improves efficiency compared to per-sample invocation schemes, computational cost remains an open concern. We provide detailed comparison of computation analysis in Appendix C.
2. **Dependence on the Underlying LLM.** Explanation quality depends on the behavior of the underlying language model. Although our ablation study shows consistent relative gains across multiple state-of-the-art LLMs, differences in generation style, inductive biases, or safety constraints may affect neighborhood construction, particularly for dialectal, low-resource, or domain-specific language.
3. **Evaluation Scale.** Our evaluation is conducted on a relatively small test set (150 instances) compared to large-scale, fully automatic explainability studies. This design choice is intentional. Unlike prior work that evaluates explanation faithfulness using model-based perturbation metrics at scale, our primary objective is to assess semantic alignment with human rationales, which requires expert annotation and careful adjudication. As human rationale annotation is costly and time-intensive, we prioritize depth and annotation quality over breadth. We note that this trade-off is common in human-centered explainability research and that our results should be interpreted as evidence of explanation quality under controlled, high-fidelity evaluation rather than as a large-scale stress test.
4. **Model and Task Coverage.** Experiments are currently limited to BERT-style discriminative classifiers on sentence-level tasks. LIME-LLM has not yet been evaluated on non-BERT architectures, generative models, or structured prediction tasks, where perturbation semantics and locality assumptions may differ.
5. **Multilingual and Code-Switched Text.** We have not yet systematically examined multilingual or code-switched inputs. Although LIME-LLM is model-agnostic in principle, neighborhood quality may vary across languages depending on LLM coverage and available linguistic resources.
6. **Scalability with Input Length.** The scalability of LIME-LLM with respect to input length remains unexplored. Our evaluation focuses on short texts; extending the approach to longer documents or paragraph-level inputs raises open questions regarding perturbation granularity, computational cost, and explanation fidelity.
7. **Locality and Global Faithfulness.** As with all local post-hoc explanation methods, LIME-LLM approximates model behavior in the vicinity of individual inputs and does not provide guarantees of global interpretability or causal faithfulness.

## Broader Impact and Ethics

Improving interpretability in NLP systems can support safer and more responsible deployment in domains such as content moderation, decision support, and policy analysis. By generating semantically coherent, on-manifold perturbations, LIME-LLM enables more faithful local explanations, helping practitioners diagnose model behavior, identify spurious correlations, and better understand model responses to sensitive language.

At the same time, post-hoc explanations carry ethical risks. Explanations may be over-trusted or misinterpreted as causal, even though LIME-LLM provides only a local approximation of model behavior. The use of LLMs for neighborhood generation may also introduce stylistic or demographic biases that affect explanation fairness, particularly across dialects or underrepresented language varieties.

More informative explanations can additionally expose sensitive content or be exploited by adversarial actors to probe or evade model behavior, es-

pecially in moderation settings. These risks underscore the need to treat explanations as diagnostic tools rather than guarantees of correctness and to pair them with human oversight and broader auditing practices.

Our evaluation involves human-annotated social media data containing toxic or offensive language, which requires careful handling and responsible release. We do not anticipate direct environmental impacts beyond those associated with standard LLM inference used during explanation generation.

## References

Josh Achiam, Steven Adler, Sandhini Agarwal, Lama Ahmad, Ilge Akkaya, Florencia Leoni Aleman, Diogo Almeida, Janko Altenschmidt, Sam Altman, Shyamal Anadkat, and 1 others. 2023. Gpt-4 technical report. *arXiv preprint arXiv:2303.08774*.

Kenza Amara, Rita Sevastjanova, and Mennatallah El-Assady. 2024. Syntaxshap: Syntax-aware explainability method for text generation. *arXiv preprint arXiv:2402.09259*.

Fabrizio Angiulli, Francesco De Luca, Fabio Fassetti, and Simona Nisticò. 2025a. Llime: enhancing text classifier explanations with large language models. *Machine Learning*, 114(12):271.

Fabrizio Angiulli, Francesco De Luca, Fabio Fassetti, and Simona Nisticò. 2025b. Llime: enhancing text classifier explanations with large language models. *Machine Learning*, 114.

Anthropic. 2025. Introducing claude sonnet 4.5. <https://www.anthropic.com/news/claude-sonnet-4-5>.

Pepa Atanasova, Jakob Grue Simonsen, Christina Lioma, and Isabelle Augenstein. 2020. **A Diagnostic Study of Explainability Techniques for Text Classification**. In *Proceedings of the 2020 Conference on Empirical Methods in Natural Language Processing (EMNLP)*. Association for Computational Linguistics.

Yi Cai, Arthur Zimek, Eirini Ntoutsi, and G. Wunder. 2023. Explaining text classifiers through progressive neighborhood approximation with realistic samples. In *2021 IEEE 8th International Conference on Data Science and Advanced Analytics (DSAA)*.

Yi Cai, Arthur Zimek, Eirini Ntoutsi, and Gerhard Wunder. 2024. **Transparent Neighborhood Approximation for Text Classifier Explanation by Probability-Based Editing**. In *2024 IEEE 11th International Conference on Data Science and Advanced Analytics (DSAA)*, pages 1–10. IEEE.

Google DeepMind. 2024. **Gemini (version 3 flash)**. Accessed: 2025-01-05.

Jacob Devlin, Ming-Wei Chang, Kenton Lee, and Kristina Toutanova. 2019. **Bert: Pre-training of deep bidirectional transformers for language understanding**. In *North American Chapter of the Association for Computational Linguistics*.

Jay DeYoung, Sarthak Jain, Nazneen Rajani, Eric P. Lehman, Caiming Xiong, Richard Socher, and Byron C. Wallace. 2019. **Eraser: A benchmark to evaluate rationalized nlp models**. In *Annual Meeting of the Association for Computational Linguistics*.

Finale Doshi-Velez and Been Kim. 2017. Towards a rigorous science of interpretable machine learning. *arXiv preprint arXiv:1702.08608*.

Qingfeng Du and Jincheng Xu. 2021. Towards a better understanding of gradient-based explanatory methods in nlp. In *International Conference on Software Engineering and Knowledge Engineering*.

Shi Feng, Eric Wallace, Alvin Grissom II, Mohit Iyyer, Pedro Rodriguez, and Jordan Boyd-Graber. 2018. Pathologies of neural models make interpretations difficult. *arXiv preprint arXiv:1804.07781*.

Alon Jacovi and Yoav Goldberg. 2020. Towards faithfully interpretable nlp systems: How should we define and evaluate faithfulness? *arXiv preprint arXiv:2004.03685*.

Mohammad N. S. Jahromi, Satya. M. Muddamsetty, Asta Sofie Stage Jarlner, Anna Murphy Høgenhaug, Thomas Gammeltoft-Hansen, and Thomas B. Moeslund. 2024. **Sidu-TXT: An XAI Algorithm for NLP with a Holistic Assessment Approach**. *Natural Language Processing Journal*.

Klaus Krippendorff. 2011. **Computing krippendorff's alpha-reliability**. In *Departmental Papers (ASC)*, University of Pennsylvania.

Orestis Lampridis, Laura State, Riccardo Guidotti, and S. Ruggieri. 2022a. Explaining short text classification with diverse synthetic exemplars and counter-exemplars. *Machine-Mediated Learning*.

Orestis Lampridis, Laura State, Riccardo Guidotti, and Salvatore Ruggieri. 2022b. **Explaining short text classification with diverse synthetic exemplars and counter-exemplars**. *Machine Learning*, 112:4289–4322.

Scott M. Lundberg and Su-In Lee. 2017a. **A unified approach to interpreting model predictions**. In *Neural Information Processing Systems*.

Scott M Lundberg and Su-In Lee. 2017b. A unified approach to interpreting model predictions. *Advances in neural information processing systems*, 30.

Binny Mathew, Punyajoy Saha, Seid Muhie Yimam, Chris Biemann, Pawan Goyal, and Animesh Mukherjee. 2021. Hateexplain: A benchmark dataset for explainable hate speech detection. In *Proceedings of the AAAI conference on artificial intelligence*, volume 35, pages 14867–14875.

Menaka Narayanan, Emily Chen, Jeffrey He, Been Kim, Sam Gershman, and Finale Doshi-Velez. 2018. How do humans understand explanations from machine learning systems? an evaluation of the human-interpretability of explanation. *arXiv preprint arXiv:1802.00682*.

Poli Nemkova, Solomon Ubani, Suleyman Olcay Polat, Nayeon Kim, and Rodney D Nielsen. 2023. Detecting human rights violations on social media during russia-ukraine war. *arXiv preprint arXiv:2306.05370*.

OpenAI. 2024. Gpt-4.1 model card and technical documentation. <https://platform.openai.com/docs/models>. Accessed: 2025-01.

Lucas Monteiro Paes, Dennis Wei, Hyo Jin Do, Hendrik Strobelt, Ronny Luss, Amit Dhurandhar, and Manish et al. Nagireddy. 2024. Multi-level explanations for generative language models. In *Annual Meeting of the Association for Computational Linguistics*.

Nils Reimers and Iryna Gurevych. 2019. Sentence-bert: Sentence embeddings using siamese bert-networks. *ArXiv*, abs/1908.10084.

Marco Tulio Ribeiro, Sameer Singh, and Carlos Guestrin. 2016. “why should i trust you?”: Explaining the predictions of any classifier. In *Proceedings of the 22nd ACM SIGKDD*.

Marco Tulio Ribeiro, Sameer Singh, and Carlos Guestrin. 2018a. Anchors: High-precision model-agnostic explanations. In *AAAI Conference on Artificial Intelligence*.

Marco Tulio Ribeiro, Sameer Singh, and Carlos Guestrin. 2018b. Anchors: High-precision model-agnostic explanations. In *Proceedings of the AAAI conference on artificial intelligence*, volume 32.

Dylan Slack, Sophie Hilgard, Emily Jia, Sameer Singh, and Himabindu Lakkaraju. 2020. Fooling lime and shap: Adversarial attacks on post hoc explanation methods. In *Proceedings of the AAAI/ACM Conference on AI, Ethics, and Society*, pages 180–186.

Richard Socher, Alex Perelygin, Jean Wu, Jason Chuang, Christopher D Manning, Andrew Y Ng, and Christopher Potts. 2013. Recursive deep models for semantic compositionality over a sentiment treebank. In *Proceedings of the 2013 conference on empirical methods in natural language processing*, pages 1631–1642.

Mukund Sundararajan, Ankur Taly, and Qiqi Yan. 2017. Axiomatic attribution for deep networks. In *International conference on machine learning*, pages 3319–3328. PMLR.

Zeren Tan, Yang Tian, and Jian Li. 2023. Glime: General, stable and local lime explanation. *Advances in Neural Information Processing Systems*, 36:36250–36277.

Giorgio Visani, Enrico Bagli, and Federico Chesani. 2020. Optilime: Optimized lime explanations for diagnostic computer algorithms. *arXiv preprint arXiv:2006.05714*.

Alex Warstadt, Amanpreet Singh, and Samuel R Bowman. 2019. Neural network acceptability judgments. *Transactions of the Association for Computational Linguistics*, 7:625–641.

Chih-Kuan Yeh, Cheng-Yu Hsieh, Arun Suggala, David I Inouye, and Pradeep K Ravikumar. 2019. On the (in) fidelity and sensitivity of explanations. *Advances in neural information processing systems*, 32.

Muhammad Rehman Zafar and Naimul Mefraz Khan. 2019. Dlime: A deterministic local interpretable model-agnostic explanations approach for computer-aided diagnosis systems. *arXiv preprint arXiv:1906.10263*.

Xingyu Zhao, Wei Huang, Xiaowei Huang, Valentin Robu, and David Flynn. 2021. Baylime: Bayesian local interpretable model-agnostic explanations. In *Uncertainty in artificial intelligence*, pages 887–896. PMLR.

Haoran Zheng and Utku Pamukszu. 2024. Scene: Evaluating Explainable AI Techniques Using Soft Counterfactuals. *arXiv.org*.

Zhengze Zhou, Giles Hooker, and Fei Wang. 2021. Slime: Stabilized-lime for model explanation. In *Proceedings of the 27th ACM SIGKDD conference on knowledge discovery & data mining*, pages 2429–2438.

Ziyu Zhou, Liya Di, Junyu Zhu, and Gaoyaguli Kader. 2025a. Pr-LIME: Two-Stage Perturbation Refinement for Phrase-Level Text Model Explanations. In *2025 IEEE 7th International Conference on Communications, Information System and Computer Engineering (CISCE)*, pages 632–635. IEEE.

Ziyu Zhou, Liya Di, Junyu Zhu, and Gaoyaguli Kader. 2025b. Pr-lime: Two-stage perturbation refinement for phrase-level text model explanations. In *2025 IEEE 7th International Conference on Communications, Information System and Computer Engineering (CISCE)*.

## A Ablation Results

### A.1 Ablation Study (Base LLM: GPT-4.1)

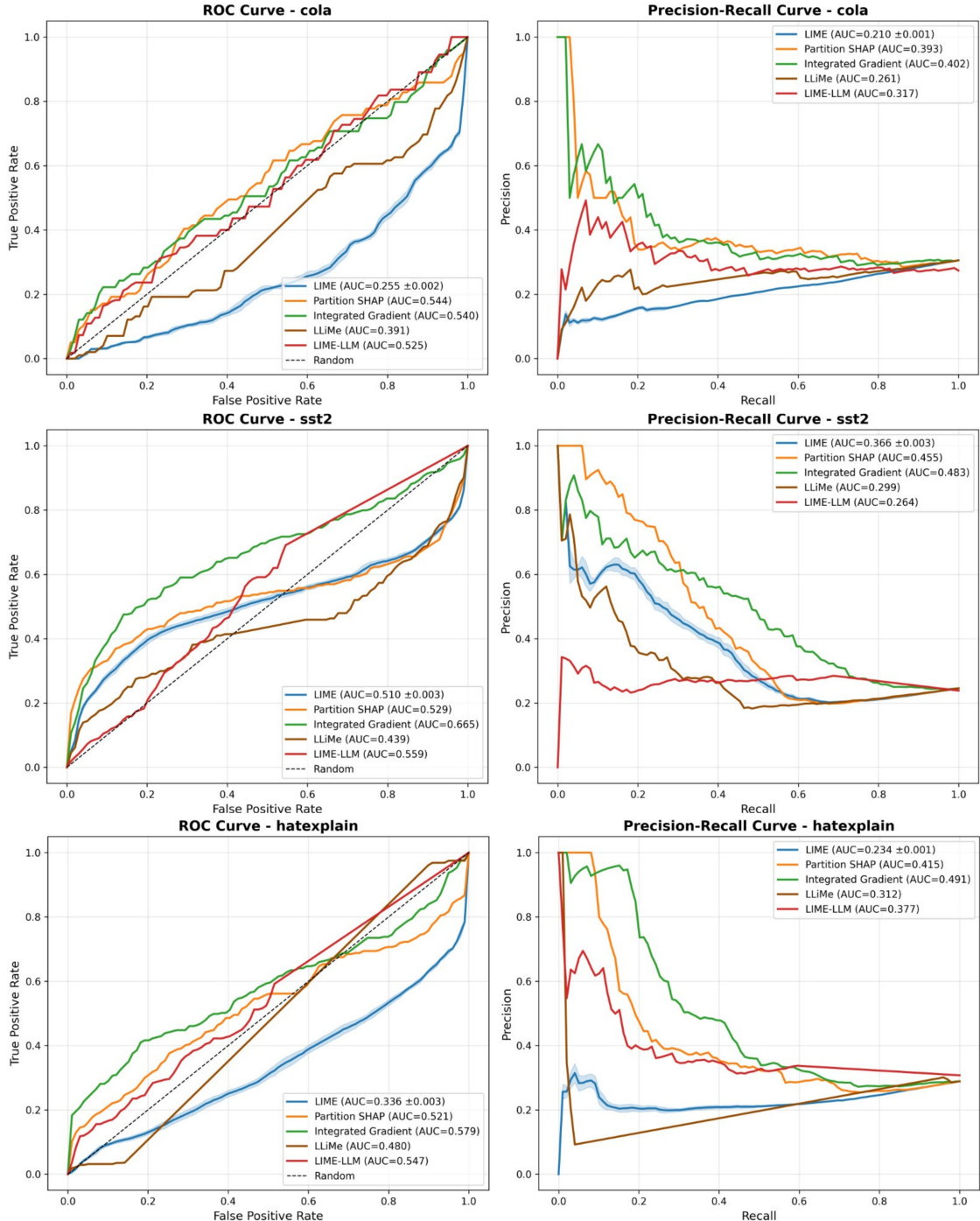


Figure 3: Ablation Study 1 (Base LLM: GPT-4.1). Comparison of ROC and Precision–Recall (PR) curves across three evaluation datasets: CoLA (top), SST-2 (middle), and HateXplain (bottom). Shaded regions denote 95% confidence intervals over 30 random seeds for stochastic methods.

## A.2 Ablation Study (Base LLM: Gemini 3 Flash)

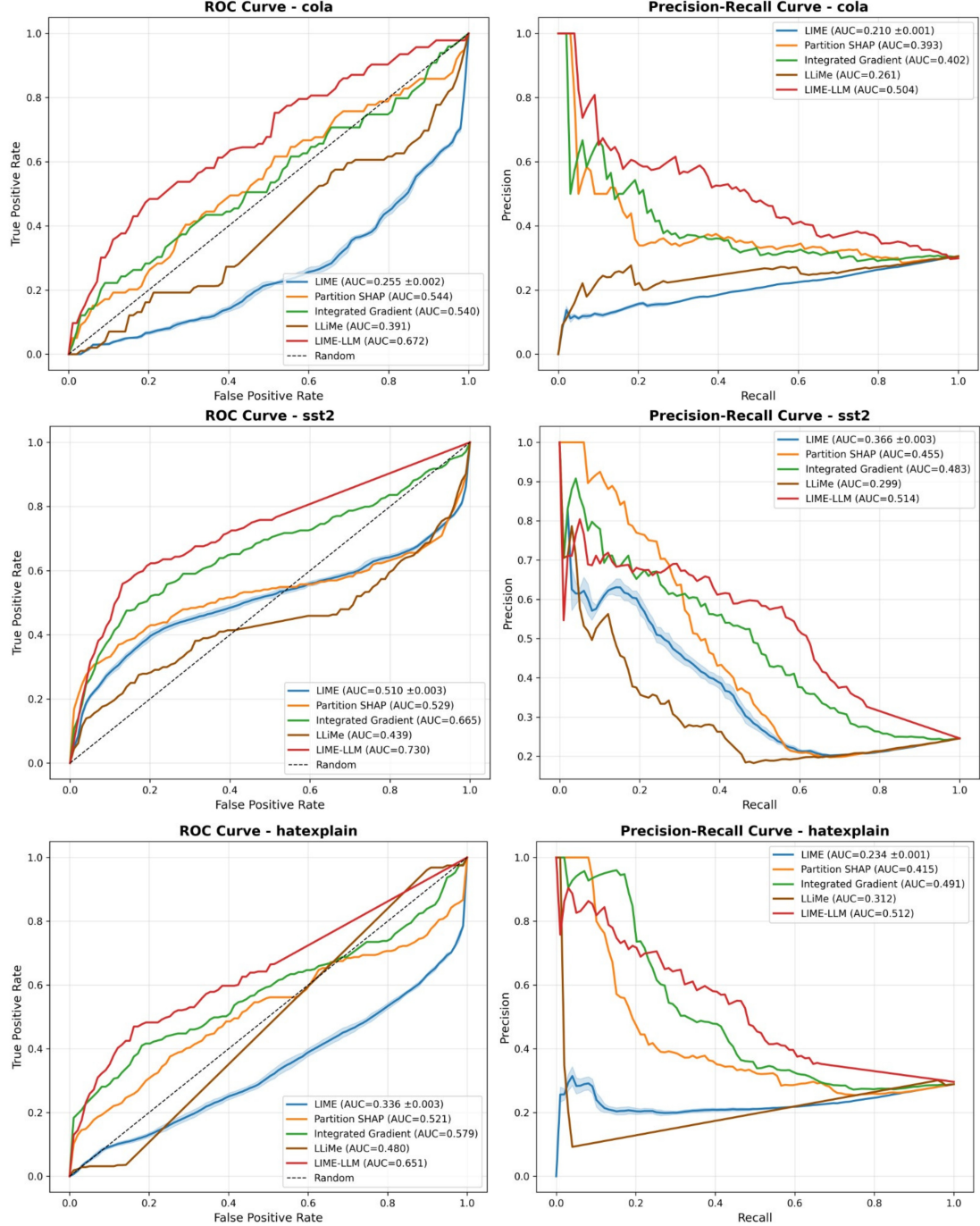


Figure 4: Ablation Study 1 (Base LLM: Gemini 3 Flash). Comparison of ROC and Precision-Recall (PR) curves across three evaluation datasets: CoLA (top), SST-2 (middle), and HateXplain (bottom). Shaded regions denote 95% confidence intervals over 30 random seeds for stochastic methods.

### A.3 Unified Ablation Table

Dataset	Backbone Model (ROC-AUC) with Hybrid Distance Metric			Distance Kernel (ROC-AUC)	
	Claude 4.5 (Main Results)	GPT-4.1	Gemini 3	BoW	Embedding
CoLA	0.598	0.578	0.544	0.622	0.587
SST-2	0.681	0.578	0.682	0.655	0.697
HateXplain	0.626	0.550	0.659	0.611	0.599

Table 3: Ablation results for LIME-LLM. **Left:** Sensitivity to the choice of LLM backbone. **Right:** Comparison of Bag-of-Words, dense embedding, and hybrid average weighting schemes. The hybrid scheme achieves the best performance; all main results (Claude Sonnet 4.5, GPT-4.1 and Gemini 3) are reported using this setting. The method demonstrates high robustness, consistently outperforming Standard LIME baselines regardless of the backbone or weighting scheme.

## B Annotation Methodology and Reliability

### B.1 LLM-Based Annotation Procedure

For SST-2 and CoLA, which lack ground-truth rationales, we employed a systematic three-stage annotation procedure using large language models:

**Stage 1: Calibration on Human-Annotated Data** To ground the procedure in verifiable signal, we calibrated on HateXplain, which provides human token/phrase-level rationales. We evaluated multiple LLMs - GPT-4o, GPT-3.5-turbo, Claude-3-5-Haiku-20241022, and Claude-3-5-Sonnet-20241022 - under several prompt variants to predict labels and highlight supporting tokens. We quantitatively compared token-level precision, recall, and F1 against the human spans. Based on this calibration, we identified Claude-3-5-Sonnet-20241022 as the most reliable annotator and established best practices for prompt engineering.

**Stage 2: Prompt Design and Validation** For SST-2 and CoLA, we curated small, manually labeled seed sets with human-annotated rationale examples (30 examples for SST-2, evenly split across classes; 30 examples for CoLA focusing on unacceptable sentences) to anchor the notion of useful token-level rationales. Guided by these examples, we iteratively refined task-specific prompts instructing the LLM to (a) predict the task label, (b) highlight tokens that justify that prediction, and (c) provide a brief explanation for their reasoning.

We developed seven prompt variants and selected the best-performing version based on the validation sets. For SST-2, the selected prompt achieved micro-F1 = 0.66 and macro-F1 = 0.69 (precision = 0.58, recall = 0.77) on identifying important tokens. For CoLA, we achieved micro-F1 = 0.88 (precision = 0.85, recall = 0.92). These figures reflect expected task differences: sentiment cues are often short and context-dependent (harder to capture consistently), whereas grammatical violations tend to be localized and more systematically recoverable.

**Stage 3: Large-Scale Annotation with Quality Controls** Using the selected prompts, we annotated the training splits at scale. To avoid propagating rationales for incorrect task predictions, we retained only instances where the LLM’s predicted label matched the gold label (label-agreement filter). We then applied light spot-checking to remove outputs with incoherent or diffuse spans. For SST-2, we limited LLM annotation to approximately 6,000 train examples due to API cost constraints. For CoLA, we annotated 2,426 training instances (primarily unacceptable examples). The final annotation counts are: SST-2 (5,971 train / 395 validation), CoLA (2,426 train / 101 validation), and HateXplain (8,042 train / 734 validation), with test sets created by splitting original validation data to ensure label balance.

Dataset	LLM	F1	Seeds	Final
CoLA	claude-3-5-sonnet	<b>0.81</b>		
	claude-3-5-haiku	0.63	30	2,426/101
	gpt-3.5-turbo	0.37		
SST-2	claude-3-5-sonnet	<b>0.69</b>		
	claude-3-5-haiku	0.68	30	5,971/395
	gpt-3.5-turbo	0.60		
HateXplain	Human	—	—	8,042/734

Table 4: LLM annotation calibration and selection results.

### B.2 Inter-Annotator Agreement Analysis

To assess the reliability and consistency of our rationale annotations, we computed Krippendorff’s Alpha (Krippendorff, 2011), a robust inter-annotator agreement coefficient that handles multiple annotators and accounts for chance agreement. For SST-2 and CoLA, we had two human annotators independently verify a subset of LLM-generated rationales on the test sets (195 examples for SST-2, 51 for CoLA). For HateXplain, we report the published inter-annotator agreement from the original dataset (Mathew et al., 2021), which involved three annotators per example.

Table 5: Inter-annotator agreement and average rationale length (K). For out experiments we limited to 50 samples each to balance the dataset across all 3 datasets and limit the cost of LLM experiment calls.

Dataset	Test Samples	$\alpha$ (Agreement)	Avg. K
CoLA	51	0.64 (moderate)	15
SST-2	195	0.84 (substantial)	3
HateXplain	726	0.46 (moderate)	9

The higher agreement for SST-2 reflects clearer sentiment-bearing tokens (e.g., “excellent”, “terrible”), while CoLA’s moderate agreement stems from linguistic nuance in grammatical judgments. HateXplain’s lower agreement is consistent with the subjective nature of hate speech annotation, where annotators may focus on different contextual cues. These agreement levels are comparable to or exceed typical values reported in rationale annotation studies (DeYoung et al., 2019), supporting the reliability of our evaluation data.

## C Computational Cost Analysis

Table 6 reports token consumption and runtime statistics for LIME-LLM and the baseline LLM across three LLM backends on the 150-instance test set.

LLM Backend	Avg. Input Token	Avg. Output Token	API Calls	Total Runtime
Claude Sonnet 4.5	844	1,806	150	57m 39s
GPT-4.1	733	1,720	150	52m 47s
Gemini 3.0 Flash	769	748	150	2h 32m
LLiMe	155	117	3,550	11h 00m

Table 6: Token usage and runtime statistics for LIME-LLM across LLM backends. Measured on 150-instance test set.